Acoustics of the avian vocal tract[a)]

N. H. Fletcher[b)] and A. Tarnopolsky
School of Aerospace and Mechanical Engineering, Australian Defence Force Academy, Canberra 2600, Australia

(Received 3 January 1998; revised 8 July 1998; accepted 22 August 1998)

The general principles underlying the acoustic performance of the avian vocal tract are examined both theoretically and experimentally. The formant resonances produced both by the total vocal tract and by the bronchial tubes are evaluated quantitatively, and their dependence upon anatomical parameters is investigated. A simplified cylindrical model for the beak is examined theoretically, and experimental results are presented that confirm the predictions of the theory for this model. A similar theoretical and experimental investigation using a more realistic conical beak model is also reported, and behaves as predicted. Finally a theoretical study of the effect of mouth volume, as influenced by tongue position, is integrated with these other studies to produce a complete analysis. The implications of these studies for understanding the acoustical behavior of avian vocal tracts are discussed. [S0001-4966(98)00912-6]

PACS numbers: 43.10.Ln, 43.80.Ka, 43.64.Tk [FD]

INTRODUCTION

Despite the existence of a very large literature on behavioral, acoustic and physiological aspects of bird song [see, for example, the classic book by Greenewalt (1968) and many more recent papers] there has been very little attempt to analyze or synthesize the behavior of the avian syrinx and vocal tract in quantitative terms. This contrasts with the situation for the human larynx and vocal tract, for which there exists a multitude of aerodynamic and acoustic studies, both analytical and synthetic. There are, of course, obvious reasons for this difference, the prime one of which is that, as humans, we have a personal interest in the functioning, or malfunctioning, of our bodies, while studies of birds are motivated largely by simple interest.

A further difficulty in the case of birds is the great variety of their anatomical dimensions and the equally large variety in the form of their vocal utterances in comparison with those of humans. For these reasons the attention paid to any particular bird species is likely to be small, and it makes sense to seek out principles and approaches that can be applied fairly generally. It is the purpose of the present paper to examine the passive acoustics of the avian vocal tract, to exhibit the new techniques that must be applied, and to present some results that are of fairly general applicability. Because the treatment is properly quantitative and formalized, it can be applied to birds with quite different anatomical dimensions simply by inserting the appropriate numbers in the calculation. This is, however, only half the story, and the acoustics of the passive vocal tract must then be considered quantitatively in relation to the active sound generation mechanism of the syrinx in the manner discussed in an earlier paper (Fletcher, 1988).

Papers on sound production in birds often emphasize the difference between birds and humans, but it is important to recognize also the similarities. In both cases the air flow is modulated by some kind of vibrating valve—a pair of vocal folds in humans and a membrane valve in the syrinx of birds—and the acoustic output of this valve passes through the vocal tract where it is inevitably modified by the resonances of this tract, which can be controlled to some extent by changing the configuration of tongue, jaw and lips in the case of humans, and of tongue and beak in the case of birds. Some human languages use whistles interpolated among voiced sounds, and all use aerodynamic noise to produce consonants; birds similarly produce voiced harmonic sounds and also more or less pure-tone whistles. A recent survey of human voice production is given in papers in the volume edited by Davis and Fletcher (1996) while Brackenbury (1982) and Casey and Gaunt (1985) have discussed the situation for birds.

The anatomy of psittacine birds resembles that of humans in that there is one vocal valve located at the junction of the bronchi and trachea, though instead of consisting of two cartilaginous fleshy folds it comprises two membranes that are brought into opposition by inflating an external air sac. The actual motion of the vocal valve is complex in each case, and involves multiple degrees of freedom, leading to wavelike motion, or at least to a phase difference between different parts of the valve structure (Ishizaka and Flanagan, 1972; Sundberg, 1987). Nevertheless, it is possible to model the behavior to a reasonable approximation by assuming a much simpler single-mass-and-spring type of motion and considering the forces exerted upon it during air flow (Fletcher, 1988).

In song birds (Oscines), in contrast, the syrinx consists of two separate syringeal valves, one in each bronchus below its junction with the trachea. Each of these is a membrane valve and can be modeled as above. Some birds use only one of these valves for singing, but some use both simultaneously, producing either the same or a different frequency (Suthers, 1990, 1994). In either case a characteristic bronchial resonance can be observed in the song.

In both birds and humans the vocal valve is character-

[a)]''Selected research articles'' are ones chosen occasionally by the Editor-in-Chief that are judged (a) to have a subject of wide acoustical interest, and (b) to be written for understanding by broad acoustical readership.

[b)]Permanent address: Research School of Physical Sciences and Engineering, Australian National University, Canberra 0200, Australia.

ized as ''pressure-controlled'' in the same sense as the reed valve of a woodwind instrument or the lips of a trumpet player. There are, however, significant differences. The reed valves of woodwinds are ''blown closed'' by the activating pressure, while the lips of a trumpet player and the vocal valves of mammals and birds are ''blown open.'' There is a simple physiological safety reason for this design. A valve that is blown open by pressure can be set into autonomous oscillation at a frequency very close to that of its mechanical resonance provided the air supply driving it comes from an enclosed reservoir (Fletcher, 1993; Fletcher and Rossing, 1998). When the output of the valve is connected to some sort of resonator, such as a pipe, there are therefore two possible situations: in both the valve oscillates at its own resonance frequency, but in the first this is set well below the frequency of the first pipe resonance, while in the second the two frequencies match, giving a strong sound with emphasis on the fundamental.

In human speech the vocal fold frequency F_0 is well below that of the first vocal tract resonance F_1, and the same is true for much voiced bird song. The vibrations of the vocal valve produce a pulsating air stream with high harmonic content at frequencies $2F_0, 3F_0, 4F_0, \ldots$, because of nonlinearity in the flow equations. The strengths of these upper harmonics in the radiated sound are then modified by the vocal tract resonances, producing vowel formants in the case of humans, and similar formants that can be recognized in Sonagraph records for bird song (Patterson and Pepperberg, 1994). In high soprano song, however, the vocal fold frequency may be comparable with that of the first, or even the second, vocal tract resonance, and the singer must adjust these resonances to match the frequency of the vocal fold vibration to produce a strong sound. The same is probably true of some varieties of bird song (Brittan-Powell *et al.*, 1997). The precise origin of ''whistled'' song, however, still remains obscure (Fletcher, 1989).

It is important to recognize the distinction between this behavior and that of the ''blown closed'' valves of woodwind reed instruments, which can be maintained in oscillation at any frequency below their mechanical resonance by coupling to a suitable acoustic resonator (Fletcher, 1979; Fletcher and Rossing, 1998). Failure to recognize this difference has caused a good deal of confusion in the literature and a false emphasis on ''coupled'' and ''uncoupled'' vocal tract resonators. The vibration of the vocal valve will lock to the resonance of the vocal tract only when the frequencies of both are nearly equal. Evidence from experiments in which birds sang after breathing an atmosphere of helium and oxygen, which has a much higher sound velocity than air and therefore raises the vocal tract resonance frequencies proportionally, convincingly supports this general picture (Nowicki, 1987; Brittan-Powell *et al.*, 1997).

The purpose of the present paper is not to explore the whole mechanism of sound production in birds, but rather simply to investigate the resonances of the vocal tract. Whether the syringeal source vibrates at a frequency nearly identical to that of a vocal tract resonance, or at some lower frequency, the vocal tract still has a major influence on the song.

Discussions of the vocal tract in the literature have generally treated the vocal tract in a grossly simplified manner, characterizing it as a simple tube that is either acoustically open at both ends, open at one end only, or even closed at both ends (Brittan-Powell *et al.*, 1997), while even a cursory anatomical study shows that none of these models can be really appropriate. At its lower end, the trachea passes through the syringeal valve, which may be either open or closed at different parts of its oscillation cycle, and is terminated by a length of bronchial tube and the abdominal air sacs. These present an acoustic impedance that can, at least in principle and probably in practice, be evaluated (Fletcher, 1988). At its upper end, the trachea passes through the laryngeal constriction to enter the mouth, and this in turn is terminated by the complex geometry of the beak. At the very least, this combination presents an end-correction to the acoustic length of the trachea that is to some extent under the control of the bird. Detailed calculations show that the vocal tract resonances may approximate those of a singly closed tube for one part of the cycle and those of a doubly open tube for another part, giving a complex set of resonances that appear also in the song of the bird modeled (Fletcher, 1988). For these reasons, we simply calculate the acoustic input impedance of the upper vocal tract at the position of the syringeal valve, recognizing this as one important component of a more complex total system.

The first section of the paper deals explicitly with song birds, and with the consequences of their having syringeal valves that lie below the junction of the bronchi with the trachea. In particular, the bronchial resonance associated with this anatomy is calculated and displayed.

The discussion in the main part of the paper, however, is common to both song birds and those species with only a single syringeal valve at the foot of the trachea, for what is calculated is the input impedance of the trachea at this point. The trachea itself is a simple tube and holds little interest, while the larynx, mouth and tongue can be modeled as a constriction and as a short tube of variable cross section, respectively. Major interest is focused upon the beak, because its complex geometry makes it difficult to analyze in a simple way, while there is ample observational evidence that beak opening is strongly correlated with song frequency (Westneat *et al.*, 1993). To give some substance to the results of the calculations, they are compared with experimental results using a large-scale model.

I. THE BRONCHIAL FORMANT

The bronchial formant seems to have been first identified in work by Suthers (1994) in the song of the oil bird *Steatornis caripensis*. This bird is peculiar in that its vocal system lacks bilateral symmetry, so that the lengths of the two bronchi, measured from the syringeal valves to the junction with the trachea, are very different. The song shows two distinct formant bands, one at about 5 kHz and one at about 8 kHz, and Suthers was able to show, by blocking first one and then the other bronchus, that these are associated with resonances of the two bronchial segments, behaving essentially as quarter-wave pipe resonators. It is our aim here to place this observation on a quantitative footing by calculat-

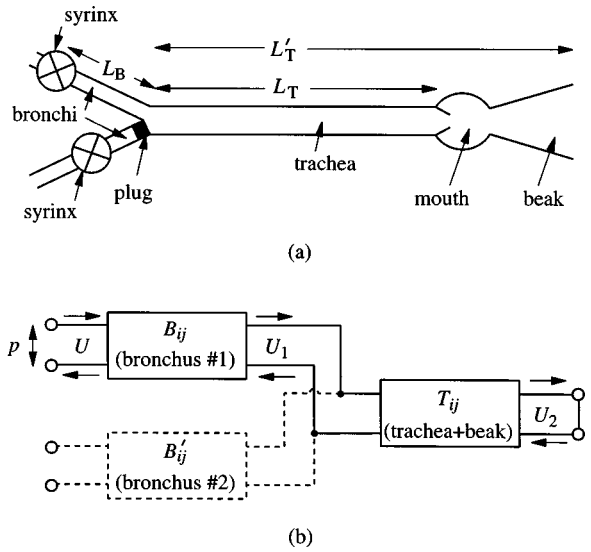

FIG. 1. (a) Model of the avian vocal tract with one blocked bronchus. The acoustic effect of the beak is taken into account by increasing the effective length of the trachea. (b) Analog network for calculation of the input impedance at the syringeal valve. When the other bronchus is unblocked, the part of the circuit indicated with broken lines becomes operative.

ing the vocal tract impedance presented to the syrinx valves. For the present we ignore the complexities of the mouth and beak, and assume the trachea to behave as a simple open tube with an appropriate end-correction to account for these.

The reason that the input impedance of the vocal tract at the syrinx valve is important is that the valve has a high impedance relative to the vocal tract, and so acts essentially as a flow source. The power that it supplies to the vocal tract is therefore proportional to the product of the vocal tract input impedance Z_V and the square of the acoustic volume flow U.

If we consider just one bronchus leading to the trachea, with the other being blocked as in the experiments of Suthers, then the vocal tract can be idealized as shown in Fig. 1(a). We simply have a bronchial tube of length L_B and cross sectional area S_B leading to a trachea of length L_T and area S_T. For simplicity in the model, we ignore for the moment the acoustic contribution of the beak and assume it to be taken into account by an adjustment of the tracheal length to a value L'_T appropriately greater than its geometric length L_T.

In Fig. 1(b) is shown the network analog from which the behavior of the system can be easily calculated, the case of one blocked bronchus involving only the circuit elements shown as full lines. Details of this approach are given by Fletcher (1992). Each tubelike element is described by a 2×2 matrix of impedance coefficients Z_{ij}, given explicitly for the case of a tube of length L and cross section S by

$$Z_{11}=Z_{22}=-j\frac{\rho c}{S}\tan kL,$$
$$Z_{12}=Z_{21}=-j\frac{\rho c}{S}\csc kL, \tag{1}$$

where ρ is the density of air, c is the speed of sound in air, $k=\omega/c+j\alpha$, $\omega=2\pi f$ is the angular frequency in which we are interested, and $\alpha\approx2\times10^{-5}(\omega/S)^{1/2}$ m^{-1} is the attenuation coefficient for sound propagation in the tube. As usual, $j=\sqrt{-1}$, and we assume SI units throughout. To avoid confusion, we shall replace Z_{ij} by B_{ij} when the coefficients refer to the bronchus, and by T_{ij} when they refer to the trachea. If we suppose p to be the acoustic pressure at the syrinx valve, U to be the flow through this valve, U_1 to be the flow from the bronchus to the trachea, and U_2 the flow out of the beak, then the network equations are

$$\begin{aligned}&B_{11}U-B_{12}U_1=p,\\&-B_{12}U+(B_{22}+T_{11})U_1-T_{12}U_2=0,\\&-T_{12}U_1+T_{22}U_2=0,\end{aligned} \tag{2}$$

which can be easily solved to give the input impedance Z_{in} as

$$Z_{\text{in}}=\frac{p}{U}=B_{11}-\frac{B_{12}^2T_{22}}{B_{22}T_{22}+T_{11}T_{22}-T_{12}^2}. \tag{3}$$

We have retained the distinction between B_{11} and B_{22} and between T_{11} and T_{22} in this analysis, so that the results apply also to the case in which the bronchus and trachea are tapering rather than uniformly cylindrical, provided we use appropriate generalizations of the impedance coefficients Z_{ij}.

It is reasonable to ask, at this stage, whether it is adequate to treat biological tubes, such as those of the vocal system, as though they have rigid walls, which is the implicit assumption underlying Eqs. (1) above. While the walls of the trachea are not particularly soft, they are certainly not ideally rigid. It is simple to include this lack of rigidity in the wave propagation equations for the tube using the formalism of Appendix B, in which the lack of rigidity of the walls simply adds a parallel element to the compressibility Y of the enclosed air. This, in turn, simply modifies the sound propagation velocity c. In practice there may be complications to the calculation because of the elastic resonance of the walls, but they are in general sufficiently thick that the correction to c, and thus to the wave number k, is much less than 10%. It is therefore reasonable to neglect this in our calculations, and in the model experiments to follow. There will also be an extra contribution to the damping coefficient α, but all this does is to slightly broaden any resonance peaks.

The expression in Eq. (3) can easily be evaluated numerically, as a function of frequency, when we insert specific values for the anatomic dimensions involved. For the case of the oil bird these dimensions are given in Table I for the two separate bronchi, and the calculated results are shown in Fig. 2. We see that each curve exhibits a number of resonances with a 1, 3, 5,..., frequency sequence, based upon a fundamental frequency of about 600 Hz. These are the resonances

TABLE I. Assumed anatomical dimensions.

	Case (a)	Case (b)
Length of trachea	100 mm	100 mm
Length of bronchus	10 mm	15 mm
Acoustic length of beak	20 mm	20 mm
Diameter of trachea	5 mm	5 mm
Diameter of bronchus	3 mm	3 mm

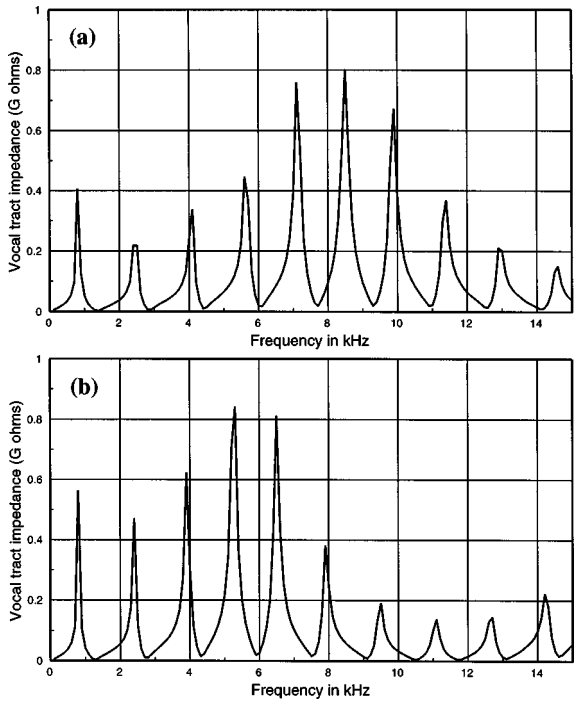

FIG. 2. Calculated vocal tract input impedance for the simple model of Fig. 1, using the anatomical dimensions given in Table I for cases (a) and (b).

of the complete vocal tract consisting of bronchus, trachea and beak. In human speech, the vocal-fold frequency F_0 is very much less than the frequency of the lowest of these resonances, and they would constitute the normal vocal formants. A bird, however, adopts a song strategy that is similar to that of a coloratura soprano singer, for whom F_0 is comparable with the frequency of the first vocal tract resonance. In this case, song is produced most efficiently if the vocal tract shape is adjusted so that one of its low resonances coincides with F_0, or perhaps its second harmonic $2F_0$.

Each curve in Fig. 2 also shows a peak in the envelope of the resonances, at about 8.5 kHz in the case of the shorter bronchus in (a) and at about 5.5 kHz for the longer bronchus in (b). This is the formant imposed by the bronchial resonance and noted by Suthers, and does indeed correspond fairly closely to a quarter-wave resonance condition of the bronchial segment between the syringeal valve and the junction with the trachea. Indeed it is interesting to note that, at this resonance, the bronchial tube constitutes a quarter-wave transformer which improves the acoustic matching between the syringeal generator and the trachea.

The fact that Eq. (3) gives a quantitative prediction of behavior allows us to examine the consequences of variations in anatomic quantities such as the lengths and diameters of the various sections of the vocal tract. Such numerical experimentation immediately establishes that a discontinuity in diameter at the junction between bronchus and trachea is essential for the production of this high formant, as we expect on acoustic grounds, since reflection is necessary to establish a resonance.

We can see the algebraic origin of these resonances quite clearly from (3). There will be peaks in the impedance Z_{in} when the denominator in the second term becomes very small so that

$$(B_{22}+T_{11})T_{22}-T_{12}^2\approx 0. \tag{4}$$

If we neglect damping by setting $\alpha=0$ in k, then B_{ij} and T_{ij} become pure imaginary and this expression can be made to vanish exactly, giving a good approximation to the resonance frequencies. If the bronchus is narrower than the trachea, so that $S_B<S_T$, then these frequencies lie a little above the values for which $\omega=(2n-1)c/4(L_T+L_B)$, that is the quarter-wave resonances of the total vocal tract length consisting of bronchus plus trachea plus beak. These are the primary vocal tract resonances.

If we are near in frequency to a quarter-wave resonance of the bronchus, then $B_{11}=B_{22}\to 0$ and $B_{12}\to Z_B$, and the second term in (3), which contains the resonance, approaches its maximum value. When the frequency is midway between these quarter-wave bronchial resonances, on the other hand, then all the $B_{ij}\to\infty$ and the two terms in (3) cancel so that the primary resonances are suppressed. This is the explanation for the shape of the envelope of the resonances in Fig. 2.

It is worthwhile to examine briefly the effect of going to the natural case in which both bronchi are open, as shown by removing the plug in Fig. 1(a). The analog network, shown in Fig. 1(b), then includes the branch shown with broken lines. This network can be solved in just the same way, and yields the result

$$Z_{\text{in}}=B_{11}-\frac{B_{12}^2(B'_{11}T_{22}+T_{11}T_{22}-T_{12}^2)}{B'_{11}(B_{22}T_{22}+T_{11}T_{22}-T_{12}^2)+B_{11}(T_{11}T_{22}-T_{12}^2)}, \tag{5}$$

where B refers to the bronchus in which we are interested (No. 1) and B' to the other bronchus (No. 2), the valve of which is assumed to be closed. (A similar expression could be deduced if we assume the other syrinx to be open.) We can see that, if the second bronchus is closed at its junction with the trachea, so that $B'_{11}=\infty$, this expression reduces to that in (3), as indeed it must.

Once again the envelope of the resonances reaches a maximum at the quarter-wave resonances of the active bronchus No. 1 and for the same reason as before. Thus although the detailed frequencies of the peaks of the impedance curve will be a little altered, it will still show a formant band at the same position as for the simple case. The same is true if the bird is using the syringeal valve in bronchus No. 2. Use of both syringeal valves simultaneously will thus produce both formants, which is what was observed by Suthers (1994).

Though the oil bird is a peculiar anatomical case, we expect similar behavior for all song birds. The distinction is perhaps that the syrinx membranes are usually located rather high in the bronchi, close to its junction with the trachea, so that the bronchial formant frequency is very high and perhaps outside the frequency range normally studied.

II. THE BEAK

As mentioned in the Introduction, acoustic analysis of the beak is made complex because of the fact that it opens along its sides for a considerable distance. This means that we must consider radiation loading on this opening, and also means that the acoustic behavior may vary in a rather com-

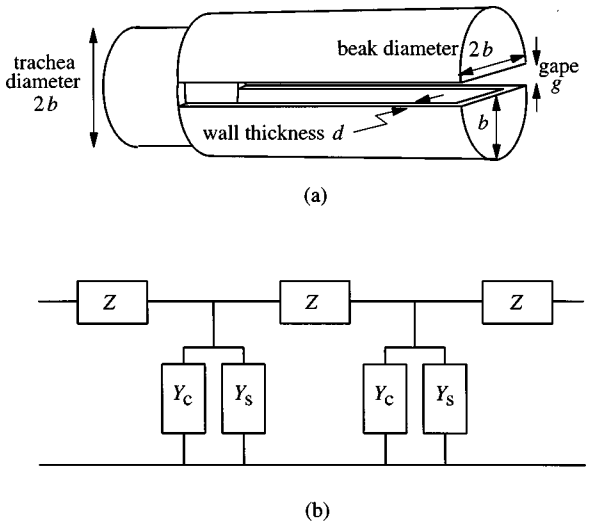

FIG. 3. (a) Simplified model of the bird beak. (b) Network analog used to calculate the behavior. The repeating sections indicate the series impedance Z and the two shunt admittances Y_c and Y_s (all per unit length) for the enclosed volume and the slit, respectively.

plex manner with beak gape. We attack this problem by a combination of theoretical analysis and direct experiment.

Clearly a rigorous model of the acoustic behavior of the beak must be three dimensional, to allow for the complex acoustic flows involved. While such an analysis could be carried out numerically, using some sort of finite element program, its results would probably not be very illuminating in a general sense, though reasonably accurate for the particular case studied. It is therefore more useful to approach the problem by constructing a model that is simple enough to solve analytically, but at the same time is sufficiently realistic to incorporate the key features of an actual beak. To this end we investigate first a very simple model and then one that is more complex and more realistic.

We should emphasize at the outset that our objective here is to obtain a reasonable understanding of the acoustic characteristics of the avian beak, rather than to carry out a precise study of the behavior of our simple models. For this reason we have been satisfied with quite modest theoretical rigor and experimental accuracy, and the results should not be judged on this basis.

A. Cylindrical beak model

Our first highly simplified model is shown in Fig. 3(a). The model is cylindrical, with uniform side openings. The major advantage of such a model is its easy geometrical description, which allows simple calculation of its acoustic behavior. We want to understand the general behavior of such a beak as a preliminary to investigating a more realistic model that is not so straightforward to analyze.

From an acoustical point of view, the beak may be regarded as a slotted transmission duct with a radiation admittance that is uniformly distributed along its length. The behavior of such a duct is characterized by its series impedance and shunt admittance, both per unit length of duct. Suppose that the series impedance per unit length of the beak at frequency ω is $Z(\omega)$. Then $Z(\omega)$ is essentially the masslike inertive load contributed by axial flow of the air in the duct, and has the value

$$Z(\omega)=R_w+j\frac{\rho\omega}{S}, \tag{6}$$

where S is the cross-sectional area of the beak, R_w is the small viscous resistance at the walls, and the other symbols have their usual meanings. Similarly, let $Y(\omega)$ be the shunt admittance per unit length of the beak. Then $Y(\omega)$ has two parts, one a compliance Y_c contributed by the compressibility of the air in the beak, and the other the admittance Y_s per unit length of the slits on each side of the beak, as shown in Fig. 3(b). We can thus write

$$Y(\omega)=Y_c+Y_s=j\frac{S\omega}{\rho c^2}+Y_s. \tag{7}$$

The beak cross-sectional area S is related to the slit width, or gape, g by

$$S=\pi b^2+2bg. \tag{8}$$

The acoustic impedance S_s of unit length of slit has two parts, Z_{flow} associated with flow between the slit walls and Z_{radn} associated with the flow transitions (radiation impedance) at the open ends of the slit. The first of these is easily evaluated (Olson, 1957, p. 89) and is approximately

$$Z_{\text{flow}}(\omega)\approx\frac{12\eta d}{g^3}+j\frac{6\rho d\omega}{5g}, \tag{9}$$

where η is the viscosity of air. The radiation impedance of unit length of a slit of width g is more difficult to calculate, but we can derive an approximate result as shown in Appendix A. If we neglect the small conductive part of the admittance, this result has the form

$$Y_{\text{radn}}\approx j\frac{\pi}{\rho\omega\ln(kg/4)}, \tag{10}$$

where $k=\omega/c$ as usual.

We can now add Z_{flow} and Z_{radn} to estimate the slit admittance Y_s per unit length along the beak. Remembering that there are two slits, and that $Z_{\text{radn}}=(Y_{\text{radn}})^{-1}$ when we deal with unit length of slit, we can write

$$Y_s\approx 2[Z_{\text{flow}}+(Y_{\text{radn}})^{-1}]^{-1}. \tag{11}$$

We can get an insight into the behavior of this beak model by neglecting the small resistive components of Z_{flow} and Z_{radn} and retaining only the imaginary parts of these expressions. We also assume that the gape g is within the range typical of bird beaks so that, as shown in Appendix A, it is a reasonable approximation to take the end correction at the slit to be $\delta\approx g$. We can then write

$$Y_s\approx -j\left(\frac{3\rho\omega d}{5g}+\frac{\rho\omega}{2}\right)^{-1}. \tag{12}$$

When we combine this with the compressive compliance Y_c of the enclosed air, as in (7), we have an expression of the form

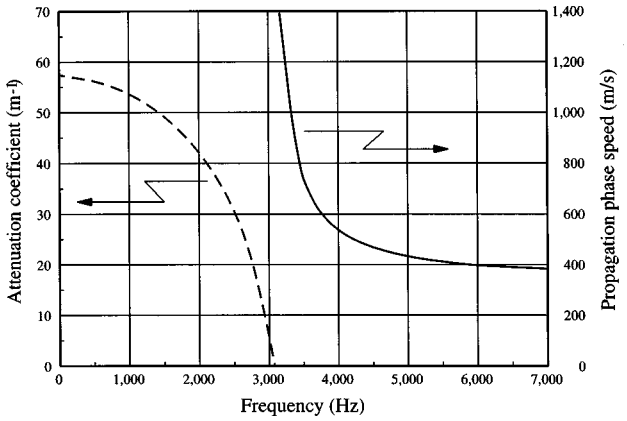

FIG. 4. Calculated behavior of the simplified beak model of Fig. 3, with beak diameter 10 mm, wall thickness 2 mm and gape 5 mm. Above the cutoff frequency $f^*=\omega^*/2\pi$, which is here about 3100 Hz, a sound wave is transmitted with phase velocity v that is greater than the normal sound velocity $c\approx 340\ \mathrm{m\,s^{-1}}$. Below f^* the wave is attenuated, and the attenuation coefficient behaves as shown.

$$Y(\omega)=j\left(A\omega-\frac{B}{\omega}\right), \tag{13}$$

where

$$A=\frac{\pi b^2+2bg}{\rho c^2}, \quad B=\left(\frac{3\rho d}{5g}+\frac{\rho}{2}\right)^{-1}. \tag{14}$$

It is clear from (13) that $Y(\omega)$ is negative imaginary for small values of ω, goes through zero, and then becomes positive imaginary, as ω increases. The frequency $\omega=\omega^*$ for which $Y(\omega)=0$ is a sort of transverse Helmholtz resonance frequency for the slotted duct, with only flow through the slit taken into account. We call ω^* the propagation cutoff frequency for the slotted beak, for a reason that will appear in a moment, and it can be calculated by setting $Y(\omega)=0$ in Eq. (13).

Returning to the transmission behavior of the slotted duct, it is easy to show from standard transmission-line theory (see Appendix B) that its characteristic impedance is

$$Z_0(\omega)=(Z/Y)^{1/2} \tag{15}$$

and that the phase speed v and wave number $k=\omega/v$ of waves in the duct are

$$v(\omega)=\omega/(ZY)^{1/2}, \quad k(\omega)=(ZY)^{1/2}. \tag{16}$$

We note that these expressions reduce to their normal forms $Z_0=\rho c/S$, $v=c$, and $k=\omega/c$ when the slit is closed, so that $g=0$, and the small contribution R_w to Z from wall losses is neglected.

From our discussion of the behavior of $Y(\omega)$ above, we see immediately that $k(\omega)$ is imaginary for $\omega<\omega^*$, so that the wave is exponentially damped as $\exp(-|k|x)$ below the cutoff frequency, rather than propagating through the slotted duct. For ω just greater than ω^*, Y is small and the phase speed v is very large, while for $\omega\gg\omega^*$ the slits have little effect and $v\approx c$. This behavior is illustrated in Fig. 4.

The behavior of the cutoff frequency with beak gape is clearly of interest. An approximate result can be derived from (13) by setting $Y=0$, and has the form

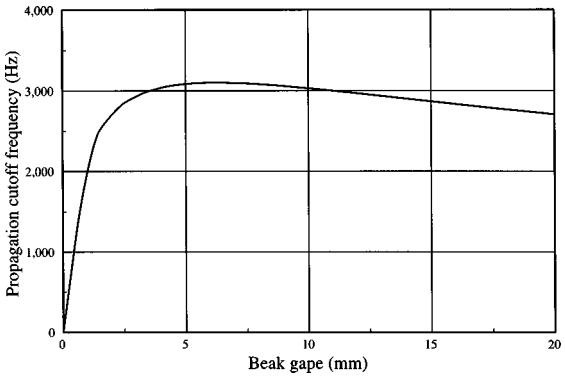

FIG. 5. Calculated propagation cutoff frequency, as a function of the gape, for a simple cylindrical beak of internal diameter 10 mm and wall thickness 2 mm.

$$\omega^*\approx\left[\frac{10gc^2}{S(6d+5g)}\right]^{1/2} \tag{17}$$

with $S=\pi b^2+2bg$ as in (8). The curve in Fig. 5 shows the general form of the behavior for a model approximating a real bird beak in dimensions. For a more accurate calculation, which is hardly justified, the logarithmic expression for the slit radiation impedance as given in Appendix A should be used, and the resulting equation solved numerically. As expected, the propagation cutoff frequency scales simply inversely with beak size, provided diameter, gape and wall thickness are all kept in proportion.

As a final theoretical exercise, it is straightforward to calculate the acoustic reactance presented by such a beak to the trachea, and from this the end correction can be evaluated. If we neglect resistive losses by radiation from the beak slits, then the impedance coefficients K_{ij} for the beak can be found from the expressions (2), simply by substituting (8) for the effective cross-sectional area and using the phase velocity v, given by (16), in place of the free propagation sound speed c. An expression for the impedance Z_K is similarly easy to derive. The input admittance of the beak is then

$$Z_{\mathrm{beak}}=K_{11}-\frac{K_{12}^2}{K_{22}+Z_K}. \tag{18}$$

When this expression is evaluated numerically, however, the behavior is dominated by longitudinal resonances of the beak cavity unless damping by radiation from the slit is included. The calculation is therefore not of much value for comparison with experiment.

B. Experimental verification

To verify these predictions, experiments were conducted using a large-scale beak model. The trachea was represented by a plastic pipe, about 1 m in length, 34 mm in internal diameter, and 4 mm in wall thickness, and the beak by an extension of this pipe formed by slitting a 100-mm-long section of it longitudinally and partly closing the remote end with two semicircular plugs. The gape opening of this model beak could be adjusted between zero and about 30 mm. The end correction, evaluated at the junction between the plain pipe and the model beak, was measured using a standing-wave tube as normally used for measuring acoustic imped-

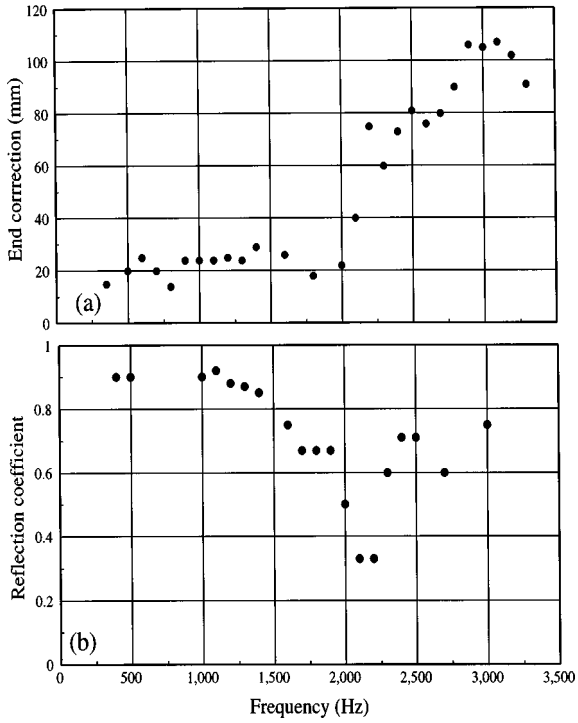

FIG. 6. (a) Measured end-correction, as a function of frequency, for the experimental cylindrical beak model with a gape of 10 mm. The calculated cutoff frequency $f^*=\omega^*/2\pi$ for sound transmission along the slotted duct is 1800 Hz in this case. Note that the end-correction is actually undefined to within a half-wavelength. (b) The measured reflection coefficient R. Note the minimum near the cutoff frequency.

ance (Beranek, 1988). The standing-wave ratio in the pipe was also measured, thus giving an indication of the losses at the beak end. Choice of the diameter of the model trachea to match that of the beak reduces complications and is easily generalized later.

The measured end-correction behaved just as expected. At low frequencies the beak presented very nearly an ''open-end'' termination to the trachea, with the actual value of the end-correction depending upon the gape but not significantly upon the frequency. This end-correction exhibited a sharp transition at about the frequency predicted by the theory, and for higher frequencies increased as would be expected for a wave propagating to the more-or-less closed remote end of the beak. This behavior is illustrated in Fig. 6(a). The value to be assigned to the end correction above the cutoff frequency is arbitrary to the extent of an added half-wavelength, and has been taken to have the smallest possible positive value for convenience.

Also of importance is the measured standing-wave ratio H, which is just the ratio of the maximum to the minimum amplitude in the trachea tube. From H we can determine the reflection coefficient R at the beak from the relation

$$R=\frac{H-1}{H+1}. \tag{19}$$

This quantity is shown in Fig. 6(b), from which it is clear that there is a minimum in the reflection coefficient, corresponding to a maximum radiation efficiency, just above the cutoff frequency. This is what we might expect, for the phase

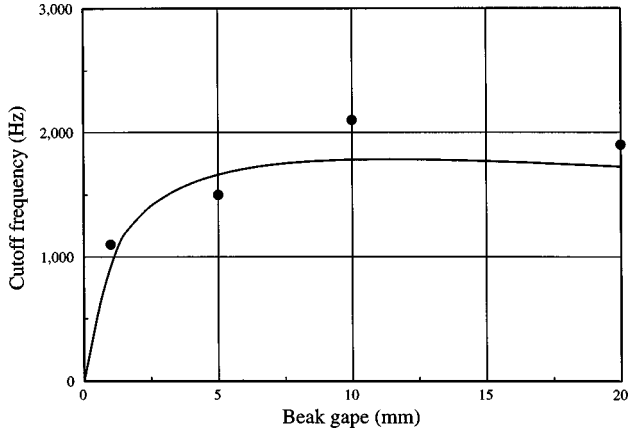

FIG. 7. Measured variation of the transmission cutoff frequency of the model beak as a function of beak gape (symbols), compared with the calculated variation of the cutoff frequency.

velocity in the beak is then high, and the two slots radiate as sources with uniform phase.

The measured variation of the cutoff frequency with beak gape is shown in Fig. 7, where it is compared with the calculated variation of $f^*=\omega^*/2\pi$ as evaluated from (17). It can be seen that the agreement is acceptably good for small gapes. For large gapes the radiation losses are so large that it is not possible to distinguish the cutoff behavior.

The next part of the experiment examined the variation of radiation directivity with frequency and beak gape. The directivity behavior measured in the horizontal plane (the plane of the slit) was simple: below the transmission cutoff frequency f^*, the radiation pattern is not far from being omnidirectional, with the 0° forward direction dominating the 180° rearward direction by only about 3 dB. Near f^* there is a transition to a more nearly figure eight pattern with a minimum in the 90° direction, and this pattern is maintained at higher frequencies. Example measurements are shown in Fig. 8. The reason for this behavior is clear. At low frequencies, the standing wave in the slotted pipe is exponentially attenuated with distance along the slot, giving two

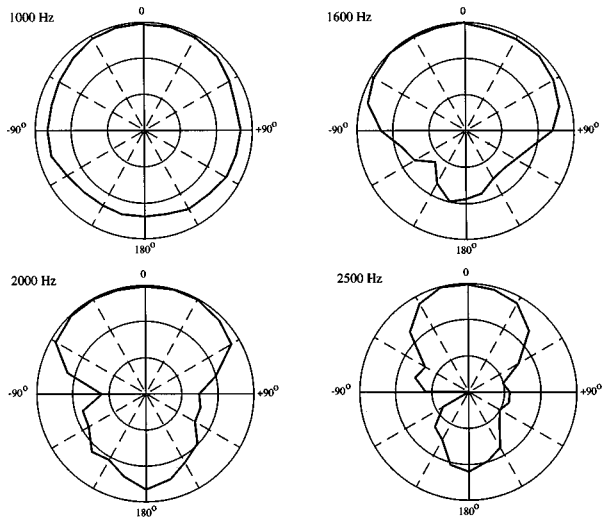

FIG. 8. Measured directivity patterns for the cylindrical model beak with a gape of 10 mm. The propagation cutoff frequency in this case is about 1600 Hz.

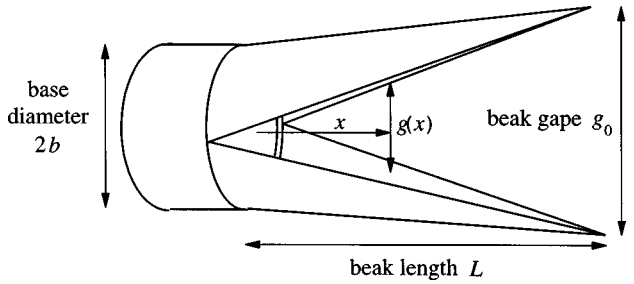

FIG. 9. A more realistic beak model, with important dimensions marked.

short slot sources separated by much less than a wavelength, so that they behave quite like a single point source. Just below the cutoff frequency, the standing wave extends along nearly the whole length of the slotted pipe, because the attenuation becomes very small, while just above cutoff the behavior is similar because the wave is transmitted and has a very high phase velocity. These two longer cophase sources are efficient radiators. At frequencies further above cutoff, however, the slotted pipe is long enough to encompass more than one half-wavelength of the standing wave, and the lateral separation between the two slit sources is also an appreciable fraction of a wavelength. This complex source has good axial radiation efficiency but low efficiency in the transverse 90° direction. When similar measurements were carried out in the vertical plane, the response on the axis was necessarily unchanged, while that at 90° increased so as to nearly eliminate the minimum, suggesting that it is the phase delay between the two slits that is primarily responsible for it.

To complete the study of this simplified model, we should examine the behavior of the transfer function between internal acoustic pressure and the total radiated sound pressure. This is essentially equivalent to evaluating the magnitude of the real part of the radiation impedance as a function of beak gape and frequency. Because the cylindrical beak model is very artificial, we shall not report this study here, but defer it for mention in relation to the conical beak model of the next section.

In relating these experimental results to the behavior of real bird beaks, it is important to correct the scaling. The model used in the experiments was larger than typical bird beaks by a fact ranging from about 3 to 10. Fortunately the scaling law is quite simple, at least to a first approximation. If we scale all geometrical dimensions similarly, say by a factor ξ, then the end correction also scales as ξ and the frequency response scales as ξ^{-1}. All the frequencies reported in our experiments should therefore be scaled upwards by a factor between about 3 and 10 for the smaller beaks of typical birds.

C. Conical beak model

While it is possible, using finite-element numerical methods, to calculate the acoustic behavior of a fairly realistic model beak, this tells us rather little about general principles. We therefore explore in a much less accurate manner the acoustics of a simplified but improved beak model. As shown in Fig. 9, this model consists of a cone, split lengthwise and opened along the split plane. For convenience the gape g_0 is defined to be measured at the tip of the beak, as shown.

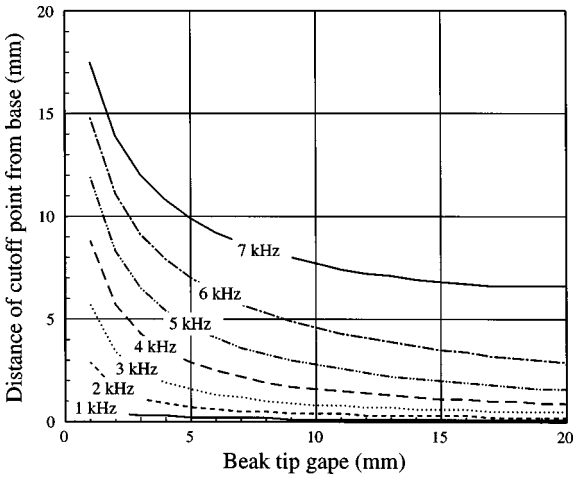

FIG. 10. Calculated distance of the cutoff position from the beak base, as a function of gape and frequency, for a beak 50 mm long, 10 mm in base diameter, and with a wall thickness 1 mm.

When we attempt to analyze the behavior of this beak model, we see immediately that a proper treatment would be quite difficult. It is, however, enough for our present purposes to proceed in a very first-order manner, using a one-dimensional slotted duct approach as before. The difference is that, in the present case, the duct has a progressively changing cross section, and the slits similarly vary in width with distance along the beak. The treatment we propose is reasonably well justified for the portion of the beak where the slit width is much less than the beak diameter, but ceases to be valid when this condition is no longer satisfied. Despite this, and in the absence of a better simple approach, it makes at least qualitative sense to extrapolate the formal results to cover the behavior of the complete beak from root to tip.

Suppose that the beak length is L, its base radius b, and its gape at the tip is g_0. Then we can approximate the local slit width $g(x)$ at a distance x from the base of the beak by

$$g(x)=g_0 x/L \tag{20}$$

and the duct cross section $S(x)$ at x by

$$S(x)=\frac{\pi b^2(L-x)^2}{L^2}+\frac{2g_0 bx(L-x)}{L^2}. \tag{21}$$

The local cutoff frequency for transmission along the duct is therefore given, in this approximation at least, by substituting these values in the treatment of the previous section.

The result of this calculation is shown in Fig. 10. The cutoff position moves towards the tip of the beak at higher frequencies, but towards the base of the beak as the gape is increased. This is just what we would expect from our discussion of the simple cylindrical beak. The numerical reliability of the calculation is, however, not high, because the assumptions upon which it is based are rather far from being satisfied—the slit is not uniform, and is not very long compared with its width, though both of these assumptions are closer to being satisfied when the gape is small. The unreal-

ity of some of the assumptions shows up at higher frequencies and larger gapes than those illustrated in the figure. At 8 kHz, for example, the solution diverges for gapes larger than about 10 mm, which suggests that the calculated x values at 7 kHz and large gapes are probably too large. Despite this, it is not unreasonable to suppose that the calculation describes the actual behavior at least qualitatively, and perhaps semiquantitatively.

We can go a little further and see what this means in terms of end-correction behavior at the beak. This is not simple, because the acoustic load past the cutoff position depends upon gape and frequency, but we can make some qualitative statements. Certainly we should expect from Fig. 10 that the end-correction will decrease as the gape is increased, and that it will decrease as the frequency is lowered. Both of these aspects of the acoustical behavior are similar to those deduced for the cylindrical beak model, but here the change with frequency is gradual, rather than having an abrupt discontinuity.

D. Conical beak measurements

A conical beak model was constructed by making a light sheet-metal cone, 200 mm in length, to fit on the end of the plastic trachea, so that its diameter at the base was about 40 mm. The cone was then slit lengthwise to make a fairly realistic beak, and hinged to the tracheal tube to make a model vocal tract. Once again, measurements of end correction and standing-wave ratio were made using a modified acoustic impedance tube. The gape g_0 was defined in this case to be the opening at the beak tip. This model is, of course, large compared with the beak of a typical bird, but the acoustic parameters we are investigating scale simply with size, provided that we also scale frequency inversely with size. For the beak of a typical large bird, the model dimensions should be reduced by about a factor of 5, and the frequency increased by the same factor.

Figure 11 shows the measured end correction to the tracheal tube, as a function of beak gape, for several frequencies in the range of interest. The important conclusion, which we were led to expect from our theoretical analysis, is that the effective end correction for a given gape is a good deal larger at high frequencies than at low frequencies. This is, as once again we expect, a general progressive behavior, rather than involving a sharp transition of the type found for our simplified cylindrical beak model. Only the results for a frequency of 2500 Hz appear anomalous. The reason for this is not clear, but the standing-wave ratio for larger gapes at this frequency is very low, making measurements rather difficult and inaccurate.

The general form of the behavior displayed in Fig. 11 is remarkably similar to that calculated from the simple theory and displayed in Fig. 10. To compare the two figures, we must remember that the calculated beak in Fig. 10 is smaller than the experimental beak by about a factor of 4 in all dimensions. We must therefore multiply all the distances in Fig. 10 by four and divide the frequencies by four for the comparison. Having done this, it is clear that there is remarkably good semiquantitative agreement between theory and experiment. It is gratifying that such a simple theory is able

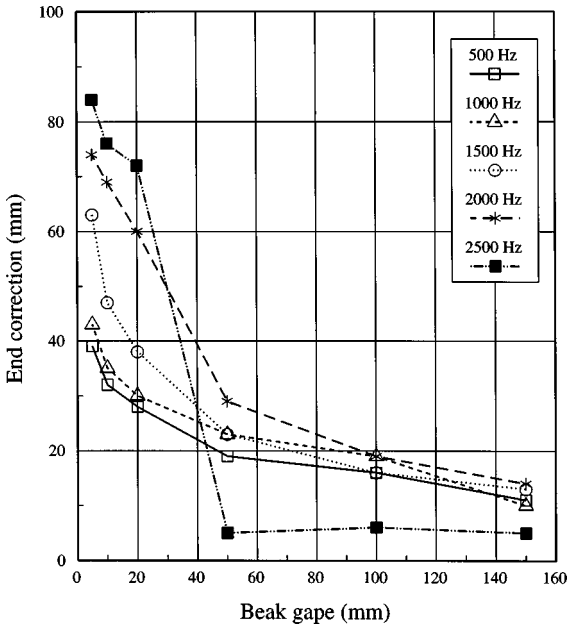

FIG. 11. Measured end correction to the trachea tube, when terminated by the tapered beak model, as a function of beak gape for a range of frequencies.

to provide such a good description of actual behavior. The fact that the experimental results become anomalous at about the same relative frequency as that at which the theory fails should not be taken to be significant.

It is useful to have an approximate expression for the end correction δ in the general case, as a function of gape and frequency. Clearly the measured end correction should scale, in both magnitude and frequency, with the size of the beak, if the geometric proportions remain similar. An empirical expression that describes the measured results and that has been appropriately scaled is

$$\delta(f,g) \approx 0.05L + 10^{-5} f L^2/g, \tag{22}$$

where L is the length of the beak and g is the tip gape, both in meters, and f is the frequency in hertz. The length to root diameter ratio of the beak is assumed to be about 6. This expression is a reasonable approximation for $g < L$, that is for a gape angle of less than about 60°, and for $f < 500/L$ numerically, but makes no claims to accuracy.

When the scaled version of this formula is compared with the theoretical results shown in Fig. 10 for the propagation distance of the wave into the beak, it is found that the end correction is about twice the propagation distance. Such a result is about what we might expect.

The next set of measurements to be made were of the radiation directivity patterns, which were made in the same way as for the cylindrical beak. In addition to their intrinsic interest, these measurements are important in relation to the radiation transfer function, as we see later. The results of these measurements, as shown in Fig. 12, are qualitatively quite similar to those for the cylindrical beak model, except that there is no pronounced ''figure-eight'' region, presumably because of the beak taper. Measurements taken in the vertical plane are very similar to those in the horizontal plane.

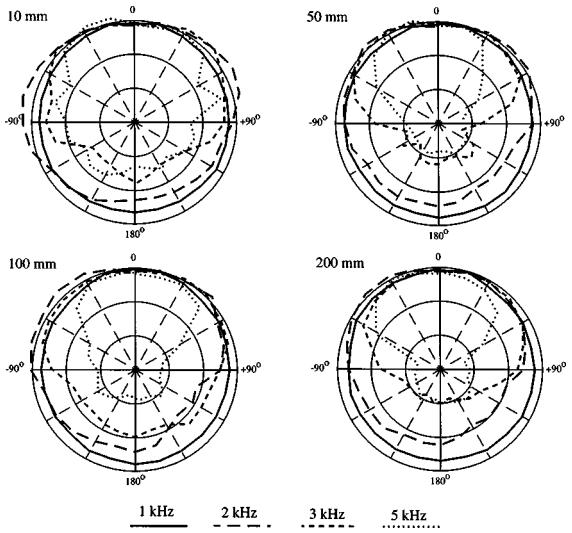

FIG. 12. Measured directivity patterns as a function of frequency and gape for the conical beak model.

Figure 13 summarizes the behavior in the form of a directional index $G(f,g)$, which we define to be the ratio, in decibels, between the measured radiated intensity on the axis and the intensity at the same distance that would be radiated by an isotropic simple source. Thus

$$G(f,g) = -10\log_{10}\left[\frac{1}{4\pi}\int_0^{\pi} 10^{0.1F(\theta)} 2\pi \sin\theta \, d\theta\right], \quad (23)$$

where $F(\theta)$ is the level at angle θ relative to the level on the axis, at the given gape and frequency. To an adequate accuracy for our present purposes, the experimental results may be approximated by

$$G(f,g) \approx 0.005 f(g+0.2) \ \text{dB}, \quad (24)$$

where g is in meters and f in hertz.

We are now in a position to evaluate the radiation transfer function for the beak. The external radiated power level is easy to define and measure. Suppose the measured root-mean-square sound pressure at a distance r on the beak axis is p_R, then the total radiated power is

$$P_R = 4\pi r^2 10^{-0.1G(f,g)} p_R^2/\rho c, \quad (25)$$

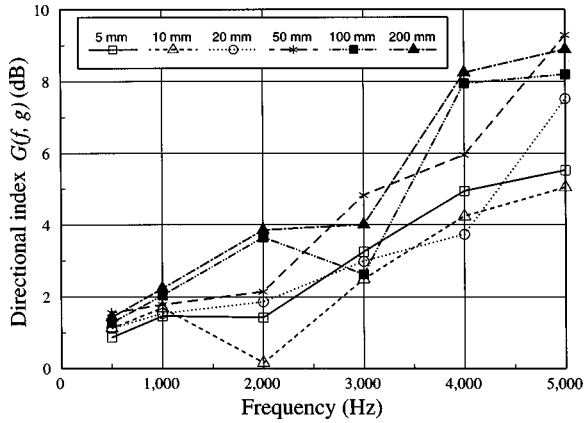

FIG. 13. Measured directional index $G(f,g)$ for the conical beak model at various gapes g, as a function of frequency f.

where the directional index $G(f,g)$, defined by (23), allows for the directivity pattern of the radiation. Internally we can most easily measure the sound pressure p_I at the pressure maxima in the standing wave pattern produced by the incident wave and the wave reflected from the beak. We can then define an internal power quantity P_I by

$$P_I = p_I^2/Z = p_I^2 S/\rho c, \quad (26)$$

where $Z = \rho c/S$ is the characteristic impedance of the trachea pipe, assumed to have area S. The justification for adopting this measure will be set out below.

Dividing these two power quantities and taking logarithms to convert the squared pressures to measured sound pressure levels L_R and L_I, respectively, relative to the same reference, we define the transfer function $T(f,g)$, in decibels, to be

$$T(f,g) = 10\log_{10}(P_R/P_I)$$
$$= L_R - L_I - G(f,g) + 10\log_{10}(4\pi r^2/S) \ \text{dB}. \quad (27)$$

The interpretation of this power transfer function is important. The radiated power P_R is clearly defined and needs no qualification. The internal power quantity P_I as defined by (26), however, can be rewritten in the form

$$P_I = U_I^2 \rho c/S, \quad (28)$$

where U_I is the volume flow amplitude at the flow antinodes in the tracheal pipe, one of which is at the beak. Since the radiated power is simply $R_R U_I^2$, where R_R is the real (resistive) part of the radiation impedance at the beak, this means that $T(f,g)$ measures, in decibels, the radiation resistance at the beak relative to the characteristic impedance $\rho c/S$ of the tracheal tube. The behavior of this radiation resistance is well known for a simple open tube, so that measurement of $T(f,g)$ allows us to evaluate the acoustic influence of the beak.

To perform the measurements, a small subtlety is required, for we do not generally know the exact location of the pressure nodes and antinodes in the model trachea, and we must evaluate the internal pressure level at a pressure maximum. To make the measurement, we therefore sealed the syrinx end of the model trachea, and inserted into it at this point a small sound source and a pressure microphone. The frequency was varied until this microphone indicated a local pressure maximum, at which point the trachea-beak system was at a resonance and the microphone was at a pressure maximum. In our experiments, actual measurement of the transfer function made use of a two-channel FFT analyzer, and the level difference $L_R - L_I$ was the envelope of the minima of the displayed transfer function.

To give a reference, we first measured the radiation transfer function for the pipe with the beak removed. This measurement should give the radiation impedance of an open tube, which is known to rise at 6 dB/oct for low frequencies and to saturate at the value $\rho c/S$, or 0 dB on our scale, for $2\pi f/ca > 2$, which corresponds here to about 6 kHz (Beranek, 1954). The measured function behaves approximately in this manner as expected, but not with great accuracy. It

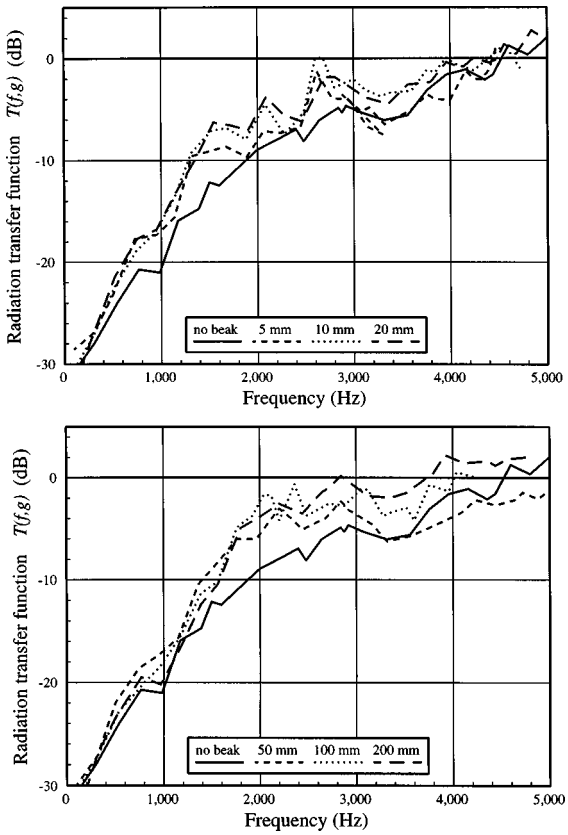

FIG. 14. Measured radiation transfer function for the conical beak model for a range of gapes. The measured transfer function for the unbaffled tracheal tube alone is shown for comparison.

can be used, however, as a reference with which the measured behavior of the beak can be compared, thus minimizing experimental errors.

Figure 14 shows the measured behavior of the radiation transfer function $T(f,g)$ for the conical beak model over a wide range of frequencies and gapes. In each part of the figure, the radiation function for the bare tube is shown for comparison. We conclude that the effect of the beak is to enhance the acoustic radiation by an amount up to about 6 dB over a limited and gape-dependent frequency range. For narrow gapes, between 5 and 20 mm, as shown in the upper part of the figure, the radiation enhancement increases with gape and occurs over the range from about 500 to 3000 Hz. For wide gapes between about 50 and 200 mm, as shown in the lower part of the figure, the enhancement once again increases with increasing gape and occurs over a range from about 1500 to 4500 Hz. When these frequencies are increased by a factor of 3 or so in order that they apply to a moderate-sized bird, it is clear that beak gape contributes a significant vocal formant to the upper parts of the song frequency range, and that this formant rises in frequency as the gape is increased. Casual listening and observation, of course, would have led one to expect this.

It is interesting to note, in passing, that the measured radiation function for the cylindrical beak model exhibits pronounced maxima, separated by about 900 Hz, above the transmission cutoff frequency, as shown in Fig. 15. These can be attributed to longitudinal half-wave resonances within the beak cavity.

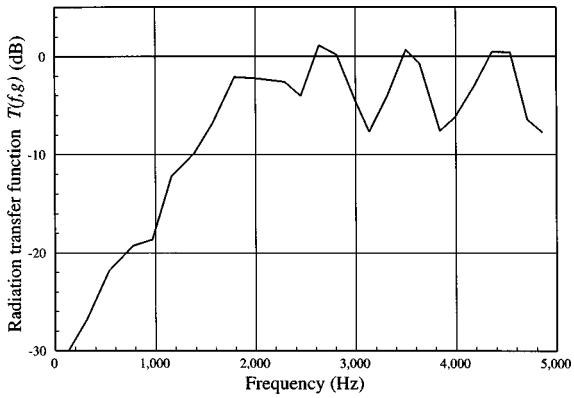

FIG. 15. Measured radiation transfer function for the cylindrical beak model for a gape of 10 mm. Note the oscillations above the transmission cutoff frequency, which is in this case about 2000 Hz.

E. Beak input impedance

Finally we need an expression for the input impedance of the beak, as seen from the mouth. A detailed solution of this problem is similar to that for a slotted, tapered waveguide or transmission line (Slater, 1942), and generally requires a numerical approach for each particular case, even given the simplifying assumptions used in our treatment. To undertake such a study would not be appropriate here, so we seek instead an approximate treatment.

The most appropriate model would seem to be to regard that part of the beak in which the sound can propagate as a short cylindrical pipe, of length equal to about half the end correction $\delta(f,g)$ given by (22), terminated by the balance of the end correction and the radiation resistance, although actually we can neglect the radiation resistance, in the interests of simplicity, because most of the acoustic damping of the system arises from losses to the walls of the narrow trachea. For the parameters of the short propagation length in the beak we could use an average of those along its length, but it is adequate to approximate these by those for the cross-section S_B and characteristic impedance $Z_B=\rho c/S_B$ at the beak root. Solving the simple network for this situation, as shown in Fig. 16(a) and detailed in Appendix C, we find for the input impedance $K(f,g)$ of the beak

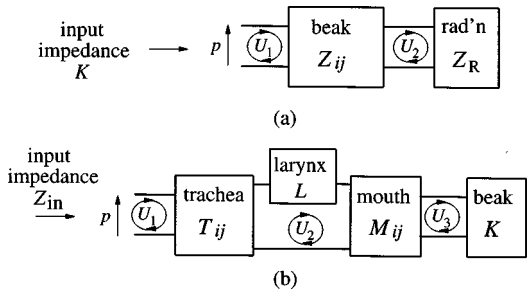

FIG. 16. (a) An approximate model for the input impedance K of the beak represents it as a tube of length $\delta/2$, described by the impedance coefficients Z_{ij}, terminated by a radiation impedance Z_R that accounts for the other half of the end correction δ. (b) The acoustic behavior of the mouth and beak can be included explicitly in the vocal-tract network of Fig. 1 by replacing the simple trachea plus mouth plus beak impedance T_{ij} by separate impedances describing trachea (T_{ij}), mouth (M_{ij}) and beak (K).

$$K(f,g)\approx jZ_B\left[-\cot\left(\frac{k\delta}{2}\right)+\frac{\csc^2(k\delta/2)}{\cot(k\delta/2)-k\delta/2}\right], \qquad (29)$$

where $k=2\pi f/c$ as usual.

From these measurements it can be concluded that the beak has a rather small overall effect on total vocal tract acoustics. Certainly it adds an end-correction, the magnitude of which varies with beak gape, but, as will be discussed below, this effect is not large. Probably more importantly, a wide beak gape increases the radiation efficiency for high frequencies by as much as 10 dB. In the model experiment this enhancement began at about 1 kHz and was greatest at about 2 kHz. Translating this a more typical bird beak of length 50 mm gives a radiation enhancement beginning at about 4 kHz and reaching a maximum of about 10 dB at about 8 kHz for a wide beak gape. This effect is certainly acoustically significant.

There are just a few reported studies in the literature that refer to the role of beak gape. One of the most thorough is that of Westneat *et al.* (1993) who examined the correlation between song frequency and beak gape for two species of sparrows, *Sonotrichia albicollis* and *Melospiza georgiana*. They found a strong and consistent correlation, with gape increasing from 10° to 50° as the song frequency increased from 3 to 7 kHz in *M. georgiana*, and a similar but smaller range in both frequency and gape in *S. albicollis*. We should expect the bird to gain several advantages from this strategy: it should be somewhat easier to align vocal tract resonances with the song frequency; the frequency shift in radiation transfer function with gape, as shown in Fig. 14 could be exploited; and the directional index, and hence audibility distance (Fig. 13), should be improved. In another study, Hausberger *et al.* (1991) examined the calls of the barnacle goose, and concluded that those with ''wide mouths'' had higher-pitched voices, a finding that is again in accord with the increased radiativity and directivity of beaks with large gape at high frequencies.

F. Vocal tract impedance

The trachea of the bird opens into the mouth at the back of the tongue through the variable constriction of the larynx. The cross-sectional area of the mouth cavity is a good deal larger than that of the trachea, but it can be modified to a considerable extent by movement of the tongue, despite its rather stiff form. The outer end of the mouth makes a transition to the beak, which we discussed in the previous section.

The acoustical behavior of the avian mouth is very similar to, though less flexible than, that of the human mouth. It functions essentially as a cavity resonator, driven from the rather high impedance of the trachea and vented by the rather low impedance of the beak. A detailed discussion cannot, however, rely upon such a simple approximation. Rather, the mouth must be considered as a short length of duct, with a diameter that can be varied by raising the tongue, inserted between the trachea and the beak. The simplified trachea plus beak impedance T_{ij} of Fig. 1 is thus replaced by the more complex combination shown in Fig. 16(b). The relevant impedances are given, once again, simply by inserting appropriate values for cross section and length in formulas (1).

TABLE II. Assumed anatomical dimensions.

Length of trachea	30 mm
Length of mouth	10 mm
Length of beak	15 mm
Diameter of trachea	3 mm
Diameter of mouth	3–15 mm
Diameter of beak root	10 mm
Beak tip gape	1–15 mm

Finally, we should include the effect of the larynx, which constricts the opening between the trachea and mouth to a variable extent. This can be represented by a simple series impedance $L=j\omega\rho l/S$, where l is the length and S the cross-sectional area of the larynx constriction, and ρ is the density of air.

The formal solution for the input impedance Z_{in} of this network at the base of the trachea is given in Appendix C, and leads to the result

$$Z_{\text{in}}=\frac{p}{U_1}=T_{11}-\frac{T_{12}^2(M_{22}+K)}{(T_{22}+M_{11}+L)(M_{22}+K)-M_{12}^2}. \qquad (30)$$

This expression can be evaluated numerically for particular combinations of effective mouth diameter, as determined by tongue position, and beak gape. We discuss some results of this calculation in the next section.

III. DISCUSSION

Now that we have set up all the formal apparatus for calculating, at least to a first approximation, the linear acoustic properties of the avian vocal tract, it is important to see where this leads us. In the present part of the discussion we omit the complicating influence of the bronchial resonances, which can be added in later for the case of song birds. We also omit the complication of a larynx constriction and assume it to be fully open.

By way of example, the calculation is made for a rather small bird with the anatomical dimensions shown in Table II. The effective diameter of the mouth has been assumed to be variable between 3 and 15 mm, the reduction in cross-sectional area, and thus in effective radius, being accomplished by raising the tongue, while the beak gape has been varied between 1 and 15 mm. To limit the number of curves to be displayed, it is further assumed that beak gape and effective mouth diameter are varied together, as seems reasonable. The results of three such calculations are displayed in Fig. 17, each curve being labeled with the effective mouth diameter and beak gape in millimeters.

The frequency range displayed is just sufficient to encompass the first three vocal tract resonances, and it is clear that the adjustments to the mouth and beak do have a significant effect. There are also effects on the resonances at higher frequencies, but their significance is not immediately apparent. The main conclusion is that the frequency of the first resonance, which would be termed F_1 for a human vocal system, is very little affected by the adjustments, though a

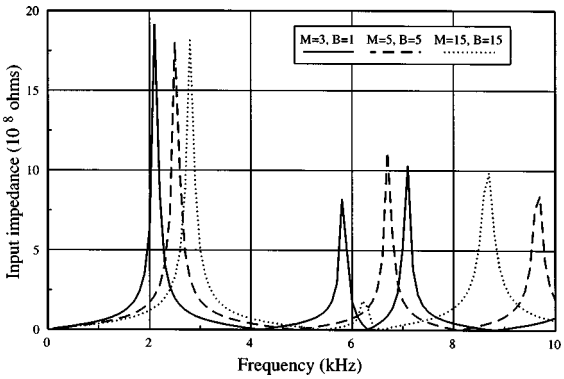

FIG. 17. Calculated vocal tract input impedance as effective mouth diameter *M* and beak gape *B*, given in millimeters for each curve, are varied. The other anatomical dimensions have the values given in Table II. The units for input impedance are 10^8 acoustic ohms, and frequencies are in kilohertz.

raised tongue and a closed beak do lower its frequency somewhat. The situation is quite different for the second and third resonances F_2 and F_3, both the frequency and height of which are considerably affected by the mouth and beak adjustments. Indeed these adjustments make it possible to position at least one resonance peak almost anywhere in the range between 5 and 10 kHz, though this resonance is sometimes F_2 and sometimes F_3. We conclude that the bird has reasonable opportunity to match a resonance to its syringeal frequency F_0 over this range, if that is the song strategy to be adopted. This does depend, however, upon the initial dimensions of the elements of the vocal tract and upon the range of variation in tongue position and beak gape that the bird can achieve.

We have not yet attempted to systematize the resonance effects illustrated in these diagrams or to check them experimentally. Such an experimental check on input impedances, using a model vocal system of the type we have employed here for the beak, is straightforward in principle, using techniques such as those developed by Benade (1960), Backus (1974), Pratt *et al.* (1977) or Wolfe *et al.* (1995) for musical wind instruments, but practical difficulties in making these measurements on live birds may be almost insuperable.

Finally, it is useful to summarize in an equation the implications of these curves and other elements that were discussed earlier. Ideally we should use a complete model in which the interaction of the vocal tract resonances on the vibrations of the syringeal valve are included (Fletcher, 1988), but for the moment it is adequate to neglect this and to consider the vibrating valve with its underlying air reservoir simply as a high-impedance acoustic source that delivers a nonsinusoidal, and therefore harmonically rich, flow to the vocal tract. If $U(f)$ is the component of this flow at frequency *f*, then the internal pressure generated at the input to the vocal tract is $p_I = Z_I(f)U(f)$ where $Z_I(f)$ is the input impedance of the vocal tract, including the bronchi as discussed in Sec. I for the case of a song bird. The total radiated acoustic power is then

$$P_I(f) = \left(\frac{\rho c}{S_B}\right) T(f,g)[Z_I(f)U(f)]^2. \tag{31}$$

This sound power is radiated with a beak formant described by $T(f,g)$ and a directionality described by the function $G(f,g)$. A similar equation applies for each harmonic component of the syringeal flow, and these can be combined to describe the radiated song, whether the syringeal frequency is closely matched to a vocal tract resonance or not.

IV. CONCLUSION

In this paper we have made a modest beginning to the quantitative exploration of the acoustics of the avian vocal system. In particular, we have confirmed the role of bronchial resonances in at least some birds, though they may not be important in all; we have elucidated the acoustic behavior of the beak in its dependence upon frequency and gape geometry; and we have shown how these elements can be combined into a model from which it is possible to make quantitative predictions about the acoustic behavior of the complete vocal tract. It is, indeed, the fact that the approach is properly quantitative to a reasonable accuracy that makes it significant—qualitative studies may be generally useful but do not provide a framework for proper testing.

Further studies—theoretical, experimental and observational—will be required in order to codify these changes in input impedance and to relate them to the acoustic strategies used by different bird species in their singing. It is not necessary for the song frequency F_0 to be rigidly tied to a vocal tract resonance frequency—indeed this is not done in human singing, except for high notes of the soprano range. Just as skilled trombone players (in whom the lips behave analogously to the syringeal valve) can play a one-octave glissando while keeping the instrument slide (and thus its resonances) fixed, or can move the slide over its full range while maintaining a steady pitch (Taylor, 1992), analogous feats should be within the capabilities of birds. There is, however, some acoustic advantage to be gained from aligning the song frequency with a vocal tract resonance, as in a musical instrument. Whatever the strategy used, however, shifts in the vocal tract resonances are bound to have a significant effect on the timbre of the resulting song.

On the basis of the results we have obtained, and the associated quantitative formulations, it should now be possible to attempt a more detailed analysis of the acoustics of bird song. The linear vocal tract resonances, of course, provide only one part of this understanding, and must be considered in combination with the nonlinear sound-production mechanism in the syrinx.

The specific graphical results presented in this paper are simply meant as examples, and do not refer to any particular species of bird. They are meant simply to indicate the typical magnitude of the effects discussed, and are certainly much more specific than mere qualitative assertions. To be really useful, however, they must be applied to the anatomy of a particular bird and compared with behavioral and acoustic data. With the aid of the formulas and equations presented in the text, such a specific application should be readily possible.

ACKNOWLEDGMENTS

This work is part of a program supported by a grant from the Australian Research Council. We are grateful to Andrew Dombek for technical support and to Martin Monteiro-Haig for assistance with some of the measurements.

APPENDIX A: RADIATION ADMITTANCE OF A SLIT

Determination of the radiation impedance at the open slots in the model beak is a complex problem. For our present purposes, however, a very roughly approximate solution is fortunately adequate, and this will now be outlined.

Provided the wavelength is long compared with the beak diameter, it is reasonable to model the right and left halves of the beak separately with each comprising a narrow slit in an infinite reflecting plane. This approximation is valid because the symmetry of the problem mandates that there is no acoustic flow across the vertical symmetry plane. We can then go further and model each slit as half of a narrow circular cylinder embedded in this plane, and the flow out of the slit as a corresponding radial dilation of the cylinder. We can then reassemble the whole into a long circular cylinder whose radius dilates at the signal frequency ω. If the length of the beak is very large compared with the width of the slit (diameter of the cylinder), then it is an adequate approximation to take this length to be infinite, and the problem then becomes one with cylindrical symmetry.

The outgoing pressure wave generated by a cylinder with radius varying at frequency ω is given by

$$p(r)=Ae^{j\omega t}[J_0(kr)-jN_0(kr)]$$
$$\approx Ae^{j\omega t}[1-(k^2r^2/4)+j(2/\pi)\ln(kr/2)], \tag{A1}$$

where J and N are, respectively, Bessel and Neumann functions, $k=\omega/c$, and A is a constant (Morse, 1954). The second form of writing is an appropriate approximation if $kr \ll 1$. This pressure wave can, in turn, be related to the displacement velocity $u(r)$ through the equation

$$\rho\frac{\partial u}{\partial t}=-\frac{\partial p}{\partial r} \tag{A2}$$

so that

$$u(r)\approx -\frac{A}{\rho c}\left(\frac{2}{\pi kr}+j\frac{kr}{2}\right)e^{j\omega t}. \tag{A3}$$

If the cylinder radius is a and the radial velocity of its surface is $u(a)$, then the acoustic admittance per unit length of slit, which is half the cylinder, is

$$Y_{\mathrm{radn}}(\omega)=\frac{\pi a u(a)}{p(a)}\approx\left(\frac{\pi a}{\rho c}\right)\frac{1}{\ln(ka/2)}\left(-\frac{\pi ka}{4}+\frac{j}{ka}\right) \tag{A4}$$

and we can relate this to the beak gape g by substituting $g/2$ for a.

This result is inaccurate for several reasons. In the first place, the length of the beak is not infinite, so that we expect the result given above to be inaccurate once the gape exceeds about one-tenth of the beak length. A second inaccuracy resides in the neglect of beak surface curvature in the immediate vicinity of the slits, this should not be a serious problem, but may introduce a systematic inaccuracy. Third, we have assumed that the slit is uniformly illuminated by an acoustic signal, with no amplitude or phase difference along its length; neither of these conditions is fulfilled at all accurately in the real situation. Despite these inaccuracies, however, the results quoted above will be sufficient to guide us in a semiquantitative manner through our analysis.

This result can be related to the effective end-correction δ to the slit length provided by the radiation load through the normal relation

$$Y_{\mathrm{radn}}=\frac{g}{j\rho\omega\delta}, \tag{A5}$$

which gives

$$\delta\approx -(g/\pi)\ln(kg/4). \tag{A6}$$

For bird beak geometries and song frequencies, kg is typically in the range 0.03–0.3, so that we expect $0.5g<\delta<2g$. In most cases it will be a reasonable approximation to take $\delta=g$.

We shall not concern ourselves with solving the case of a slit of finite length, but a qualitative remark is in order. The factor $1/\ln(kg/4)$ in the radiation admittance, and hence the reciprocal of this in the end-correction δ, derives essentially from the progressive change in propagation phase from different parts of the slit to the region of interest. If the slit length L is large compared with g but short compared with the sound wavelength, then $\ln(kg/4)$ should be replaced by a factor of order $\ln(g/L)$, which thus eliminates the apparent divergence of δ at low frequencies.

APPENDIX B: SLOTTED DUCT EQUATIONS

Here we derive briefly the two important results (15) and (16). In a network analog, electric potential takes the place of acoustic pressure, electric current takes the place of acoustic volume flow, and the duct becomes a transmission line. Suppose this transmission line has series impedance Z per unit length and shunt admittance Y per unit length. Then, for a current flow U, the change in voltage (pressure) over a very short length dx of line is

$$dp=-ZU\,dx. \tag{B1}$$

Similarly, if the pressure at the point considered is p, then the change in current over the length dx is

$$dU=-Yp\,dx. \tag{B2}$$

These two equations can be combined to give

$$\frac{\partial^2 p}{\partial x^2}=YZp \tag{B3}$$

which has the solution $p=ae^{\pm\gamma x}$ where $\gamma=(YZ)^{1/2}$. If both Y and Z are positive imaginary quantities, as they are, for example, in a simple lossless acoustic duct, then $\gamma=jk$ and the solution represents two waves traveling in opposite directions with phase velocity

$$v=\omega/k=\omega/(YZ)^{1/2}. \tag{B4}$$

We can find the characteristic impedance of an infinite line or duct by supposing that there is a small loss so that there is no reflected wave. Then $p = ae^{-\gamma x}$, and from the first equation above we find that $\gamma p = ZU$, so that the impedance of the infinite line, which is its characteristic impedance, is

$$Z_0 = p/U = Z/\gamma = (Z/Y)^{1/2}. \tag{B5}$$

APPENDIX C: UPPER VOCAL TRACT

Referring to the network of Fig. 16(a) and following the procedures given in Fletcher (1992), we can write the equations for the beak as

$$\begin{aligned} p &= Z_{11}U_1 - Z_{12}U_2, \\ 0 &= -Z_{21}U_1 + (Z_{22} + Z_R)U_2, \end{aligned} \tag{C1}$$

where the impedances Z_{ij} refer to a pipe of length $\delta/2$ and cross section S_B, and $Z_R = j\rho\delta/2S_B$ is the radiation reactance associated with the other half of the end-correction. From these equations, the beak input impedance K is

$$K = \frac{p}{U_1} = Z_{11} - \frac{Z_{12}^2}{Z_{22} + Z_R}. \tag{C2}$$

Inserting specific values for the impedances from (1), the results quoted in the text are obtained.

Similarly, using the network of Fig. 16(b) for the complete vocal tract, we can write the equations

$$\begin{aligned} p &= T_{11}U_1 - T_{12}U_2, \\ 0 &= -T_{12}U_1 + (T_{22} + M_{11} + L)U_2 - M_{12}U_3, \\ 0 &= -M_{12}U_2 + (M_{22} + K)U_3. \end{aligned} \tag{C3}$$

The solution is straightforward, and leads to the result

$$Z_{\text{in}} = \frac{p}{U_1} = T_{11} - \frac{T_{12}^2(M_{22} + K)}{(T_{22} + M_{11} + L)(M_{22} + K) - M_{12}^2} \tag{C4}$$

which can be evaluated numerically for particular values of the geometrical parameters.

Backus, J. (**1974**). ''Input impedance curves for the reed woodwind instruments,'' J. Acoust. Soc. Am. **56**, 1266–1279.

Benade, A. H. (**1960**). ''The physics of woodwinds,'' Sci. Am. **204**, 145–154.

Beranek, L. L. (**1954**). *Acoustics*, reprinted 1986 (Acoustical Society of America, Woodbury, New York), p. 122.

Beranek, L. L. (**1988**). *Acoustical Measurements* (Acoustical Society of America, Woodbury, New York), pp. 309–328.

Brackenbury, J. W. (**1982**). ''The structural basis of voice production and its relationship to sound characteristics,'' *Acoustic Communication in Birds*, edited by D. E. Kroodsma and E. H. Miller (Academic, New York), Vol. 1, pp. 53–73.

Brittan-Powell, E. F., Dooling, R. J., Larsen, O. N., and Heaton, J. T. (**1997**). ''Mechanisms of vocal production in budgerigars (Melopsittacus undulatus),'' J. Acoust. Soc. Am. **101**, 578–589.

Casey, R. M., and Gaunt, A. S. (**1985**). ''Theoretical models of the avian syrinx,'' J. Theor. Biol. **116**, 45–64.

Davis, P. J., and Fletcher, N. H. (editors) (**1996**). *Vocal Fold Physiology: Controlling Complexity and Chaos* (Singular, San Diego).

Fletcher, N. H. (**1979**). ''Excitation mechanisms in woodwind and brass instruments,'' Acustica **43**, 63–72; addendum, Acustica **50**, 155–159 (1982).

Fletcher, N. H. (**1988**). ''Bird song: A quantitative acoustic model,'' J. Theor. Biol. **135**, 455–481.

Fletcher, N. H. (**1989**). ''Acoustics of bird song—Some unresolved problems,'' Comments Theor. Biol. **1**, 237–251.

Fletcher, N. H. (**1992**). *Acoustic Systems in Biology* (Oxford U.P., New York), pp. 121, 178–203 and 309–311.

Fletcher, N. H. (**1993**). ''Autonomous vibration of simple pressure-controlled valves in gas flows,'' J. Acoust. Soc. Am. **93**, 2172–2180.

Fletcher, N. H., and Rossing, T. D. (**1998**). *The Physics of Musical Instruments*, 2nd ed. (Springer-Verlag, New York), Chap. 13.

Greenewalt, C. H. (**1968**) *Bird Song: Acoustics and Physiology* (Smithsonian Institution, Washington, DC).

Hausberger, M., Black, J. M., and Richard, J.-P. (**1991**). ''Bill opening and sound spectrum in barnacle goose loud calls: Individuals with 'wide mouths' have higher pitched voices,'' Anim. Behav. **42**, 319–322.

Ishizaka, K., and Flanagan, J. L. (**1972**). ''Synthesis of voiced sounds from a two-mass model of the vocal cords,'' Bell Syst. Tech. J. **51**, 1233–1268.

Morse (**1954**).

Nowicki, S. (**1987**). ''Vocal tract resonances in oscine bird sound production: Evidence from birdsongs in a helium atmosphere,'' Nature (London) **325**, 53–55.

Olson, H. F. (**1957**). *Acoustical Engineering* (Van Nostrand, New York).

Patterson, D. K., and Pepperberg, I. M. (**1994**). ''A comparative study of human and parrot phonation: Acoustic and articulatory correlates of vowels,'' J. Acoust. Soc. Am. **96**, 634–648.

Pratt, R. L., Elliott, S. J., and Bowsher, J. M. (**1977**). ''The measurement of the acoustic impedance of brass instruments,'' Acustica **38**, 236–245.

Slater, J. C. (**1942**). *Microwave Transmission* (McGraw-Hill, New York), pp. 69–78.

Sundberg, J. (**1987**). *The Science of the Singing Voice* (Northern Illinois U.P., DeKalb).

Suthers, R. A. (**1990**). ''Contributions to birdsong from the left and right sides of the intact syrinx,'' Nature (London) **347**, 473–477.

Suthers, R. A. (**1994**). ''Variable asymmetry and resonance in the avian vocal tract: A structural basis for individually distinct vocalizations,'' J. Comp. Physiol. A **175**, 457–466.

Taylor, C. (**1992**). *Exploring Music* (Institute of Physics Publishing, Bristol), p. 138.

Westneat, M. W., Long, J. H., Hoese, W., and Nowicki, S. (**1993**). ''Kinematics of birdsong: Functional correlation of cranial movements and acoustic features in sparrows,'' J. Exp. Biol. **182**, 147–171.

Wolfe, J., Smith, J., Brielbeck, G., and Stocker, F. (**1995**). ''A system for real time measurement of acoustic transfer functions,'' Acoustics Australia **23**, 19–20.